Topological Analysis of Chemical Bonding in Cyclophosphazenes

Victor Luaña,* A. Martin Pendás, and Aurora Costales

Departamento de Química Física y Analítica, Facultad de Química, Universidad de Oviedo, 33006-Oviedo, Spain

Gabino A. Carriedo and Francisco J. García-Alonso

Departamento de Química Orgánica e Inorgánica and Instituto de Investigación Enrique Moles, Facultad de Química, Universidad de Oviedo, 33006-Oviedo, Spain

Received: December 11, 2000

Chemical bonding in the cyclophosphazenes is studied from the point of view of the quantum theory of Atoms in Molecules (AIM). To that end, HF/6-31G** ab initio calculations are done on a collection of $(NPX_2)_3$ derivatives for a wide set of $-X$ substituents, and its electron density, $\rho(\vec{r})$, and pair density, $\rho^{(2)}(\vec{r}_1,\vec{r}_2)$, are obtained and analyzed. The $(NP)_3$ ring geometry and bonding properties are basically maintained along the cyclotriphosphazenes. The PN distance and the bond critical point properties (electron density, Laplacian, etc.) lie between those of $XNPX_3$, formally a double NP bond, and those of X_2NPX_4, formally a single NP bond, being much closer to the former than to the latter. The Laplacian of the electron density shows the PN bond to be highly polar, with a clear tendency of the P atoms to lose almost all of their five valence electrons, and a significant concentration of charge along the PN line, even though within the N basin. The charge on the ring N basins, $Q(N)$, remains almost invariant, $-2.3\ e$, in all cyclotriphosphazenes, whereas the charge of the ring P basin, $Q(P)$, varies from $+2.9$ to $+4.0\ e$, depending on the electronegativity of the $-X$ group. There is an inverse correlation between $Q(P)$ and the PN distance, the more electronegative $-X$ groups shrinking the $(NP)_3$ ring more, even though only slightly. The partition of the pair densities indicates that some 0.63 electron pairs are shared between each P and its two N neighbors in the ring, this value being typical of a polar but largely ionic bonding situation. The three N atoms in the ring share 0.20 electron pairs per N−N group, a small but significant amount, even though no bond path line occurs linking them. The three-dimensional contour surfaces of $\nabla^2\rho$ clearly depict the molecular regions having a Lewis basic or acidic character. Ring N atoms behave as weak Lewis bases, whereas ring P atoms are preferred sites for a nucleophilic attack tending to remove, perhaps ionically, a $-X$ group. These topological properties do explain the chemistry of cyclophosphazenes and agree well with the available experimental densities. The AIM analysis supports the main conclusions from the traditional Dewar's model of phosphazenes.

I. Introduction

Our aim in this article is to provide the rigorous description of the topological and bonding properties of the wave function of a large collection of cyclophosphazene compounds.

Hexachlorocyclotriphosphazene and its polymeric derivative, obtained upon heating, have a long history[1−3] since first synthesized in 1834 by Liebig, Wöhler, and Rose from the reaction of ammonium chloride and phosphorus pentachloride. The synthesis of $(NPCl_2)_n$ was much improved by R. Schenk and G. Römer in 1924 and their method remains the basis for present day bulk production. The observed formation of an entirely inorganic polymer produced a large interest at the time, suddenly lost due to the fast degradation (hydrolysis) of the polymer under ambient conditions. A second period of development was started when Allcock and colleagues demonstrated the stabilization of the compounds by attaching to the phosphorus atoms several organic functional groups. We are now under the realm of a third wave of interest, fueled by the technological aplications of the hundreds of polymeric phosphazenes synthesized so far: from elastomers to glasses, from insulators to electrical conductors, from water-soluble to highly hydrophobic compounds, from inert to bioactive materials. Polyphosphazenes are, as a matter of fact, the largest class of inorganic macromolecules.[4−7] This technological usefulness together with the unusual reactivity of the PN group has induced a realm of theoretical work in recent years.[8−14]

The P−N bond is one of the most intriguing in chemistry and many of its more subtle aspects still await for a satisfactory explanation. Limiting ourselves to the phosphazene compounds, some of the experimental facts to be accounted for include:[15] (a) ring and chain compounds are very stable; (b) all P−N distances in the $[PN]_n$ rings are equal in the $[PNX_2]_n$compounds; (c) P−N distances are significantly shorter (∼1.58 Å) than those found in saturated phosphazanes (∼1.77 Å); (d) the N−P−N angle is constant in most rings ($120 \pm 2°$) in sharp contrast with the P−N−P angle (120−150°); (e) ring N atoms can act as weak Lewis bases; (f) many reactions of the phosphazenes involve the nucleophilic attack on the P, removing one of its substituents; and (g) the phosphazenes lack the vis/UV spectral band that characterize the polyolefinic compounds.

Traditionally, bonding in the cyclic phosphazenes has been interpreted, within the Valence Bond Orbital framework, in terms of Dewar's island model.[16] Similarly to the C−C bond in the benzene ring, the P−N bond in the phosphazene ring is described as resonance between two main Lewis structures: **1** and **2** in the next scheme.

10.1021/jp0044577 CCC: $20.00
Published on Web 05/03/2001

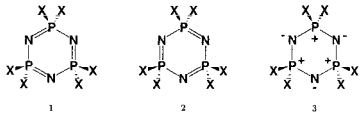

This would result in an bond order intermediate between single and double, and it would explain that all P−N bonds in the ring are identical. Different from benzene, however, the phosphazene ring shows no evidence of ring current nor any other signs of aromaticity. Dewar proposed that the ring valence charge should be heavily concentrated and anchored to the N atoms, rather than spread and flowing through the ring. The reason behind this could be attributed to the charge transfer from P to N atoms due to the difference in electronegativity between them. In the same line, it can be anticipated that Lewis ionic structures like **3** in the above diagram should have a significant participation in the molecular bonding.

How large is this participation? Where is the charge localized in the phosphazenes? How many electron pairs are shared in the P−N bond? Those are examples of the questions that can be answered through the rigorous analysis of the molecular wave function.

The rest of the article is organized as follows. A short review of the main concepts behind the quantum theory of Atoms in Molecules as used in the article is presented in the next section, followed by a description of the techniques used in our calculations. Section IV presents the bulk of this paper and it is divided into the dicussion of the phosphazene geometry, the analysis of the topological properties of the electron density, and the bonding description provided by the pair density and the spacial distribution of the Laplacian of the electron density. The article ends with the presentation of our main conclusions.

II. Theory

The atoms in molecules (AIM) theory[17−33] provides the rigorous solution to the problem of partitioning every molecular property into atomic or functional group contributions. Atoms and functional groups do exist in the same real three-dimensional space than the molecules themselves. Dividing arbitrarily a molecule into fragments gives rise, however, to the fundamental problem that many observables become ill-defined, the kinetic energy being the simplest example. It is only by selecting fragments enclosed by surfaces such that the flux of the electron density gradient is zero at every point

$$\vec{\nabla}\rho(\vec{r}_s)\cdot\vec{n}(\vec{r}_s)=0, \qquad (1)$$

that all observables become well defined and all quantum mechanical laws are fulfilled within the fragments as they are for the whole molecule.[19] In eq 1, $\rho(\vec{r})$ is the molecular electron density, $\vec{r}_s$ is a point on the zero flux surface (ZFS) that separates two fragments, and $\vec{n}(\vec{r}_s)$ is the normal vector to the surface at that point.

Equation 1 is neither arbitrary nor capricious but a direct consequence of the quantum mechanics principles when applied to the purpose of dividing the molecular space.[19,20] The partition appears, then, as a consequence of the topology of the electron density gradient vector field $\vec{\nabla}\rho$, and the localization and characterization of its critical points $\vec{r}_c$, such that $\vec{\nabla}\rho(\vec{r}_c)=\vec{0}$, becomes the first step in the analysis of bonding. Critical points can be classified according to the electron density curvature, i.e., to the eigenvalues of the Hessian matrix $\mathbf{H}=\vec{\nabla}\otimes\vec{\nabla}\rho(\vec{r}_c)$, by attending to their rank (number of nonzero eigenvalues) and signature (number of positive minus number of negative eigenvalues). This is shown in Table 1 to facilitate our discussion.

TABLE 1: Critical Points of the Electron Density Classified by Its Rank *r* and Signature *s*, as Well as the Dimensions of Its Attraction and Repulsion Basins (AB and RB, Respectively)[a]

(*r*, *s*)	AB	RB	AIM name	description
(3,−3)	3D	0D	nucleus (n)	local maximum
(3,−1)	2D	1D	bond (b)	first-order saddle
(3,+1)	1D	2D	ring (r)	second-order saddle
(3,+3)	0D	3D	cage (c)	local minimum

[a] Only the non-degenerate critical points, i.e., those with rank $r = 3$, should occur in an ordinary molecule, the presence of a degenerate point indicating structural instability.

The attraction basin of a given critical point is created by the field lines that move upward following the gradient of the electron density until reaching that point. In a similar way, repulsion basins are formed by following downward the $\vec{\nabla}\rho$ field lines. Zero flux surfaces do appear, in fact, as any of (a) the bidimensional attraction basin of a bond critical point, (b) the two-dimensional (2D) repulsion basin of a ring critical point, and (c) a symmetry mirror plane. The most significant, from a chemical point of view, are the 2D bond attraction basins, which receive the name of interatomic surfaces (IAS). Local maxima of the electron density occur at the nuclear positions in the molecule, and the boundary that separates the three-dimensional (3D) attraction basin of a nucleus from that of its neighbors is made of IAS. The nuclear critical point plus its 3D attraction basin Ω constitutes an *atom within the molecule*. Atomic properties are obtained by integrating the quantum mechanical operators in the basin,[19] and they contribute additively to the properties of the molecule. The properties of an atom or functional group can, in addition, be transferred among similar molecules. Basins with identical geometry would contribute identically to the molecular properties, even in different molecules.

As we have discussed, the 2D attraction basin of a bond critical point is the interatomic surface separating two atoms. The one-dimensional (1D) repulsion basin of the bond point, on the other hand, constitutes the *bond path*, i.e., the unique gradient vector field line that connects the two nuclei. The occurrence of a bond path between two nuclei is a necessary and sufficient condition of bonding between them.[34] The set of bond paths forms the chemical graph of the molecule[29] which, through the AIM theory, becomes an observable property rather than an empirically assumed construct. Molecular bonding, on the other hand, can be classified by attending to the properties of the electron density at the bond critical point.[28]

The Laplacian of the electron density at a point, $\nabla^2\rho(\vec{r}_s)$, measures whether the electron density is locally concentrated ($\nabla^2\rho < 0$) or depleted ($\nabla^2\rho > 0$) there, and provides a detailed map of the basic and acidic regions, respectively, of the molecule.[35] In a typically covalent bond, a region of negative Laplacian would include the bond path together with the two bonded nuclei. Prototypical ionic bonds, on the contrary, would exhibit spherical shells of basic character on each nucleus, the bond critical point occurring in a region of acidic character. Between both extreme cases we can find a collection of *polar bonding* situations showing mixed signs.

On the other hand, Lewis' concept of electron pairing[36] can be quantitatively determined[37−39] by analyzing the electron pair density,

$$\rho(2)(\vec{r}_1,\vec{r}_2) = \binom{N}{2} \int \ldots \int |\Psi(\vec{x}'_1,\ldots\vec{x}'_N)|^2 \times \delta(\vec{r}'_1 - \vec{r}_1)\delta(\vec{r}'_2 - \vec{r}_2)\mathrm{d}\vec{x}'_1\ldots\mathrm{d}\vec{x}'_N \quad (2)$$

The average number of distinct electron pairs shared between two atoms *A* and *B* in the molecule is given by the double integration of $\rho^{(2)}(\vec{r}_1,\vec{r}_2)$ such that one electron is integrated to the basin of A and the other to the basin of B:[40]

$$D_2(\mathrm{A,B}) = \int_\mathrm{A} \mathrm{d}\vec{r}_1 \int_\mathrm{B} \mathrm{d}\vec{r}_2 \rho^{(2)}(\vec{r}_1,\vec{r}_2). \quad (3)$$

Were the electrons perfectly localized into the atomic basins, D_2(A,B) should be equal to N(A)N(B)/2, where:

$$N(\mathrm{A}) = \int_\mathrm{A} d\vec{r}_1 \rho(\vec{r}_1) \quad (4)$$

is the average number of electrons within the basin of A. Electrons, however, do participate in the bonding between basins. The quantity

$$F(\mathrm{A,B}) = 2D_2(\mathrm{A,B}) - N(\mathrm{A})N(\mathrm{B}) \quad (5)$$

provides a measurement of the extent to which the electrons in *A* are delocalized into the basin of B, and vice versa.[40] Immediately from here, the *delocalization index*

$$\delta(\mathrm{A,B}) = -F(\mathrm{A,B}) - F(\mathrm{B,A}) \quad (6)$$

gives the *number of electron pairs shared between the basins* A *and* B. A related quantity

$$\lambda(\mathrm{A}) = |F(\mathrm{A,A})| \le N(\mathrm{A}) \quad (7)$$

constitutes the *atomic localization inde*x and it gives *the average number of electrons localized in the basin of A*. The difference between λ(A) and *N*(A) is due to the electrons that participate in the bonding between A and the other basins in the molecule. The localization λ(A) and delocalization indices δ(A,B) give information that complements, and is not simply contained in, the electron density.

This short brief of the rigorous ideas behind AIM theory should make clear that much can be won by completing the topological analysis of the phosphazenes wave functions.

III. Computational Procedure

The calculations discussed in this work have been done at the Hartree−Fock (HF) level using a 6-31G** standard basis set. The *GAMESS* code[41] was used to optimize the geometry, with no symmetry restrictions, and determine the wave function for the electronic ground state of the molecules involved. The topological analysis of the molecular wave functions was performed using Bader's laboratory AIMPAC package.[42] Significant illustrations were done with the help of *molden*,[43] *tessel*,[44] *POVray*,[45] and *Geomview*.[46]

The 6-31G** basis set used through this work was selected after carefully checking the geometry and bonding properties of several small molecules containing the P═N bond group. Table 2 presents the main results obtained for $HNPH_3$. Some interesting facts deserve attention. The minimal basis set, STO-3G, predicts a P−N distance 0.3−0.4 Å too short, a very large deviation compared to the typical good distances found in most CHON molecules with this basis.[47] Including polarization functions in the basis set (particularly *d* basis functions for P) is very important as it lowers 0.1−0.2 Å the P−N distance (and some 5−20° the P−N−P angles in the phosphazene ring). Diffuse basis functions are, however, not significant for the ground-state properties studied here. The differences among 6-31G** and 6-311G** or larger bases are rather small, so the former were used because of economy reasons. Correlation effects, examined in second-order Møller−Plesset (MP2) as well as in single and double excitation configuration interaction (CISD) calculations, change only slightly the equilibrium geometries and bonding properties, but increase heavily the computational effort, and they have been neglected in the remaining calculations.

TABLE 2: Basis Set and Correlation Effects on the P−N Distance *R*(P−N) and the Topological Properties of the P−N Bond Critical Point in $HNPH_3$[a]

calculation	basis set	*R*(P−N)	ρ_b(P−N)	$\nabla^2\rho_b$(P−N)
HF	STO-3G	1.209	0.099	0.085
HF	3-21G	1.668	0.162	0.320
HF	3-21G**	1.529	0.214	1.341
HF	6-31G	1.698	0.159	0.025
HF	6-311G	1.670	0.167	0.129
HF	6-31+G	1.706	0.157	0.003
HF	6-31G**	1.547	0.218	1.062
HF	6-31+G**	1.550	0.218	1.041
HF	6-311+G**	1.546	0.222	0.992
MP2	6-31G**	1.572	0.212	0.906
CISD	6-31G**	1.562	0.208	0.941

[a] Distance is given in angstroms; electron densities and laplacians in au.

TABLE 3: Main Geometrical Parameters for Several Cyclotriphosphazene Derivatives[a]

−*X*	R_{PN}	R_{PX}	∠PNP	∠NPN	∠*XPX*	ref
−H	1.582	1.388	123.09	116.91	100.99	
−F	1.564	1.533	123.44	116.56	98.67	
	(1.560)	(1.521)	(120.4)	(119.4)		69
	(1.569)	(1.525)	(121.0)	(119.0)	(98.6)	70
−Cl	1.577	2.000	123.76	116.24	102.77	
	(1.581)	(1.993)	(121.4)	(118.4)	(101.3)	71
$-CH_3$	1.601	1.814	124.31	115.70	103.65	
	(1.606)	(1.810)	(122.6)	(116.8)	(102.6)	72
$-NH_2$	1.598	1.668	122.78	117.22	106.81	
	(1.60)	(1.65)	(122.9)	(115.9)	(103)	73
−CN	1.578	1.594	124.54	115.46	103.50	
−SH	1.588	2.107	125.30	114.70	107.27	
$-CH_3$	1.578	1.583	124.39	115.61	108.23	
−OH	1.575	1.594	124.54	115.46	103.50	
−NC	1.572	1.656	123.65	116.35	100.55	
$-SiH_3$	1.617	2.274	124.04	115.96	108.79	
$-BH_2$	1.617	1.957	124.71	115.29	102.89	
$-PH_2$	1.603	2.222	123.61	116.39	103.46	
−CNO	1.580	1.758	123.69	116.31	101.33	
−NCS	1.575	1.641	123.92	116.08	100.92	
	(1.58)	(1.63)	(121)	(119)	(100)	74
−SCN	1.587	2.127	125.45	114.55	119.26	
$-N_3$	1.577	1.685	124.27	115.73	110.23	
−Br	1.579	2.164	123.87	116.13	103.62	
	(1.57)	(2.16)	(122)	(117)	(102.4)	75−77
$-CHCH_2$	1.600	1.809	124.97	115.03	113.68	
−CCH	1.586	1.767	123.84	116.16	101.76	
$-NHNH_2$	1.595	1.658	128.02	111.98	107.27	

[a] Experimental results, where available, are given in parentheses. Distances and angles are given in angstroms and degrees, respectively.

IV. Results and Discussion

A. Geometry of the Cyclotriphosphazene Ring. We will start by considering the geometry of the cyclotriphosphazene ring. Table 3 presents the equilibrium geometry of 21 cyclotriphosphazene derivatives $[NPX_2]_3$. All the compounds have a planar ring configuration, with six identical PN distances in the range 1.591 ± 0.026 Å and PNP angles (124.04 ± 1.26°) slight but consistently larger than the NPN angles (115.96 ± 1.26°).

TABLE 4: HF/6-31G Equilibrium Geometries of the X_mNPY_n Family of Compounds[a]**

	ij	R_{ij}	*ijk*	α_{ijk}
$NPCl_2$	PN	1.470	ClPCl	103.48
	PCl	2.000	NPCl	128.26
$ClNPCl_3$	PN	1.539	ClNP	118.78
	NCl	1.709	ClPCl	101.67,105.40(2×)
	PCl	1.980	NPCl	107.22,117.95(2×)
Cl_2NPCl_4	PN	1.714	ClNCl	107.53
	NCl	1.711	ClNP	126.24
	PCl	2.133(2×), 2.045(2×)	ClPCl	88.40(4×), 173.48,121.20
			NPCl	93.26(2×),119.40(2×)

[a] Distances and angles are given in angstroms and degrees, respectively.

Even though the nature of the -*X* substituent groups included in the sample is quite diverse, the ring geometry is very constant. As a contrast, the *XPX* angle shows a much higher variability: 103.73 ± 5.06°. The theoretical geometries do agree with the available experimental data to about 0.01 Å and 1−2°.

Just like the ethane-ethene-ethyne series are useful to understand the CC bond in benzene, we can examine the X_m-NPY_n family to better grasp the PN bond properties. Table 4 describes the equilibrium geometry of several compounds in this family. It can be seen that the PN distance in the phosphazene rings lies between the values found in $XNPX_3$ (formally a double NP bond) and those in X_2NPX_4 (formally a single NP bond), being much closer to the former than to the later.

B. Chemical Graph and Bonding Properties. The bond and ring critical points of the cyclophosphazenes and Cl_mNPCl_n compounds are presented in Tables 5−7. Figure 1 depicts the contour levels of the Laplacian on two planes of the $[NPCl_2]_3$-molecule. Overimposed in these plots are the repulsion and attraction basins of the bond critical points lying on each plane. Figure 2, on the other hand, presents the equivalent plot for the Cl_mNPCl_n molecules. Several significant aspects of the PN bonding in the cyclophosphazenes are readily obtained from here. First, the electron density is large at the PN bond critical point, (b(PN): 0.19−0.21 e/bohr^3). This large value lies between the PN bond density of $ClNPCl_3$ (a phosphazene) and that of Cl_2NPCl_4 (a phosphazane), being much closer to the former than to the latter.

The PN bond densities follow, in fact, a definite trend, decreasing exponentially as the PN distance increases (See Figure 3). The law $A\exp(-\alpha R)$ with $A = 3.965$ e/bohr^3 and $\alpha = 1.880$ Å^{-1} can be obtained from a least-squares fit to the data in Tables 5 and 7. The existence of a relationship between bond length and bond density for a given pair of atoms in different compounds was pointed out by Bader et al.[48] for the CC bond in hydrocarbons and later extended by Boyd et al.[49,50] and Gibbs et al.[51,52] to other atom pairs. These works assumed either a linear[48] or power law relationship. It was later discussed[53] that the exponential law $\rho_b = Ae^{\alpha R}$ provides the right behavior at the short and long-range limits and it can be explained as being inherited from the properties of the radial density of the free atoms. The exponential correlation has been also found on a very careful analysis of the experimental electron densities on hydrogen bonds.[54]

The PN bond ellipticity $\epsilon_{||} = 1 - \lambda_2/\lambda_1$ is 4−9% in the cyclophosphazenes, significantly smaller than the values found for $NPCl_2$ (15%), $ClNPCl_3$ (23%), and Cl_2NPCl_4(9.5%). As it happens for benzene, the *soft* axis (i.e., the eigenvector associated with λ_2) is perpendicular to the $[NP]_3$ ring, which is an indication of a relative charge concentration in the ring plane. Large values of the bond ellipticity have been shown to occur in two different situations: (a) multiple bonds with a significant contribution from the π-like density and (b) molecules accumulating a significant stress that moves the bond critical point out from the interatomic straight line. The last case is easily seen to occur in $ClNPCl_3$ (see Figure 2). Neither large ring stress nor large π bonding appear to be working on the cyclotriphosphazenes.

The Laplacian at b(PN) is positive and large (0.68−1.04 e/bohr^5), typical from a closed shell bonding situation. The same is concluded from the very large curvature of the density perpendicular to the interatomic surface ($\lambda_\perp$: 1.44−1.80 e/bohr^5). The Laplacian scalar field in Figures 1 and 2 shows, however, a large concentration of charge along the PN bond (a feature usually associated with covalency), even though it occurs within the N atoms basins. In fact, the atomic valence shell of the P atoms has dissappeared in the phosphazenes. In agreement with this, the bond critical point is considerably closer to the P atom (1.15−1.18 bohr) than to the N atom (1.81−1.88 bohr). In other words, N is bigger than P in the phosphazenes. We must conclude that the PN bond is strong, highly polarized, and involves a large transfer of charge from P to N.

The charge transfer can be determined quantitatively by integrating the electron density on the atomic basins:

$$Q(\Omega) = Z_\Omega - \int_\Omega \rho(\vec{r})\mathrm{d}\vec{r} \qquad (8)$$

where Z_Ω is the atomic number of the nucleus in the Ω basin. The results are collected in Table 8. The charge on N remains almost constant, −2.3 e, for the cyclotriphosphazenes. The charge on P varies significantly with the functional group attached to the phosphazene ring: 2.9−4.0 e. We can observe that the identity of the atom directly linked to the phosphorus almost determines Q(P). Thus, Q(P) is 3.7−3.8 e when P is linked to a C atom, 3.9−4.0 e when linked to a N atom, and 2.8−2.9 e when linked to a S atom. In fact, the Cahn−Ingold−Prelog ordering of the ligand groups makes clear that the charge on the phosphorus increases monotonically within each period as the attached atom becomes heavier. We can recognize here a dependency of the charge transfer with the difference in electronegativity between the atoms directly linked. On the other hand, by comparing the geometries in Table 3 with the topological charges, we can see a clear trend: the PN ring distance tends to decrease as the charge on P increases. The effect is, in any case, small.

Table 6 contains a large wealth of information regarding the ligands and their attachment to the cyclotriphosphazene ring. Among the first thing to notice is the large variability in the size of the phosphorus atom as measured by the distance from the P nucleus to the P−X bond critical point. Thus, r(P) ranges from 1.160 bohr in the P−F bond path to 2.855 bohr in the P−Si path. The variation is not arbitrary but r(P) monotonically decreases within each period as the ligand atom directly bonded to the ring becomes heavier. A large variability is also observed on the P−X bond densities, 0.103−0.183 e/bohr^3, and the $\lambda_\perp$ curvature, 0.059−2.089 e/bohr^5. The latter shows a regular trend within each period, whereas the former presents a more involved evolution. The value of the Laplacian at the bond critical point is, on the other hand, negative for the bonding between P and the H, B, P, S, and Br atoms, and positive for the bonding of P to C, N, O, F, Si, or Cl atoms. This is clearly related to the relative electronegativity of the bonded atoms: a small difference in electronegativity produces covalent bonding with negative Laplacian, whereas a large difference gives rise to

TABLE 5: Critical Point (CP) Properties of Several Cyclotriphosphazenes: Only Bond (*b*) and Ring (*r*) CPs Situated on the $(NP)_3$ Ring Are Given in This Table[a]

$-X$	CP	r_i/r_j	ρ	$\nabla^2\rho$	$\lambda_\perp$	$\epsilon_\parallel$ (%)	G
$-H$	b(PN)	1.176/1.814	0.207928	0.679309	1.447562	8.13	0.345992
	r		0.021180	0.102030	−0.011856	0.00	0.023644
$-BH_2$	b(PN)	1.177/1.880	0.187687	0.816947	1.436960	11.29	0.343321
	r		0.017515	0.090256	−0.010630	0.00	0.019816
$-CH_3$	b(PN)	1.168/1.860	0.194431	0.890053	1.555923	7.70	0.367646
	r		0.018418	0.096347	−0.011779	0.00	0.021073
$-CHCH_2$	b(PN)	1.167/1.858	0.195560	0.896339	1.565013	7.29	0.371178
	r		0.018672	0.097834	−0.011285	0.00	0.021454
$-CCH$	b(PN)	1.160/1.839	0.201324	0.945405	1.641577	7.37	0.390060
	r		0.019031	0.101634	−0.012291	0.00	0.022063
$-CN$	b(PN)	1.157/1.826	0.204527	0.981508	1.688253	7.57	0.402376
	r		0.019579	0.104792	−0.012904	0.00	0.022692
$-CNO$	b(PN)	1.157/1.830	0.204163	0.969614	1.676720	7.27	0.399638
	r		0.019414	0.104029	−0.012655	0.00	0.022537
$-NH_2$	b(PN)	1.164/1.851	0.198550	0.911846	1.604447	3.82	0.378811
	r		0.018720	0.098324	−0.012818	0.00	0.021322
$-NHNH_2$	b(PN)	1.163/1.853	0.199492	0.911384	1.600944	8.81	0.381308
	r		0.018561	0.102785	−0.011078	0.00	0.022369
$-NC$	b(PN)	1.153/1.819	0.208712	1.005518	1.738195	6.24	0.414270
	r		0.019849	0.107921	−0.013404	0.00	0.023301
$-NCS$	b(PN)	1.154/1.823	0.208006	0.993306	1.724021	6.06	0.410859
	r		0.019653	0.106953	−0.013130	0.00	0.023096
$-N_3$	b(PN)	1.155/1.826	0.206792	0.986929	1.709759	6.44	0.407209
	r		0.019646	0.106024	−0.012923	0.00	0.023013
$-OH$	b(PN)	1.153/1.824	0.207907	0.996812	1.732318	6.45	0.410811
	r		0.019584	0.107080	−0.013399	0.00	0.023136
$-OCH_3$	b(PN)	1.155/1.828	0.207127	0.978568	1.710587	5.70	0.406196
	r		0.019393	0.105796	−0.013242	0.00	0.022854
$-F$	b(PN)	1.148/1.807	0.212634	1.044815	1.798671	5.69	0.428118
	r		0.020298	0.111612	−0.014851	0.00	0.023916
$-SiH_3$	b(PN)	1.177/1.880	0.187320	0.826139	1.439110	11.28	0.344527
	r		0.017584	0.089156	−0.011501	0.00	0.019584
$-PH_2$	b(PN)	1.171/1.860	0.192424	0.881972	1.521253	10.05	0.363158
	r		0.018095	0.094556	−0.011728	0.00	0.020589
$-SH$	b(PN)	1.162/1.841	0.199472	0.945869	1.619775	9.79	0.387014
	r		0.018790	0.102099	−0.011842	0.00	0.022139
$-SCN$	b(PN)	1.162/1.838	0.199878	0.953391	1.624614	9.70	0.389438
	r		0.019018	0.103255	−0.011596	0.00	0.022428
$-Cl$	b(PN)	1.156/1.824	0.204819	0.992612	1.693011	8.17	0.404964
	r		0.019435	0.105655	−0.013090	0.00	0.022766
$-Br$	b(PN)	1.158/1.827	0.203397	0.979179	1.669401	8.77	0.400147
	r		0.019256	0.104608	−0.013029	0.00	0.022546

[a] The atomic radius along a bond path, r_i, is defined as the distance from the nucleus to the bond CP. In the case of bond CPs $\lambda_\perp = \lambda_3$ and $\epsilon_\parallel = 1 - \lambda_2/\lambda_1$, where $\lambda_1 \le \lambda_2 \le \lambda_3$ are the eigenvalues of the Hessian matrix. In the case of ring CPs, however, $\lambda_\perp = \lambda_1$ and $\epsilon_\parallel = 1 - \lambda_2/\lambda_3$. Perpendicular and parallel refer to the plane tangent to the 2D attraction (repulsion) basin of the bond (ring) critical point. All properties are given in au.

charge transfer among the basins and a positive Laplacian at the bond critical point.

Some of the ligands exhibit, on the other hand, unusual bonding properties: (a) the $-CHCH_2$, $-NHNH_2$, and $-OCH_3$ cyclotriphosphazenes have bond paths between the closest hydrogens in two adjacent ligand groups; (b) similarly, the $-N_3$ and $-SCN$ compounds present N−N and C−C bond paths between the two side chains in each P; and (c) the acetylene group shows a nonnuclear maximum in the middle between the two C atoms. The occurrence of a bond path between the ligands is an extreme case of a common phenomenum. In effect, as we will examine later, the geometry of the ligands, and particularly the *XPX* angle, is determined by the close contact between the ligand basins. The P basin, however, is large enough to avoid a real contact between the ligands, except in a few cases. Cioslowski et al.[55] have related the presence of such long distance bonds between same sign ligands to "steric overcrowding". Bader,[56] however, has demonstrated that bond paths do always appear because their existence diminishes the total energy of the molecule and, thus, bond paths do not reveal molecular instability. Nonnuclear maxima of the electron density, on the other hand, have been shown to be a normal step in the formation of a bond between two equivalent atoms if examined at the appropriate distance.[57] The equilibrium distance of the acetylene group lies in the upper limit of the range of apparition of a nonnuclear maximum between two C atoms.

The large polarity of the PN bonding represents a big difference between the $[PN]_3$ and the benzenic ring. All six carbons in benzene lie in a toroidal region of negative Laplacian. When a magnetic field is applied perpendicularly to the molecule, the electrons flow easily from C to C originating a ring current.[58] This should not be the case in the cyclophosphazenes, and aromaticity should not be expected here. This is exactly what Jemmis and Kiran[59] have obtained in the calculation of the aromatic stabilization energy (ASE), defined as the energy of the reaction:

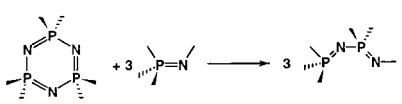

TABLE 6: Properties of the Bond Critical Points of the Electron Density of Several Cyclotriphosphazene Derivatives[a]

−X	CP	r_i/r_j	ρ	$\nabla^2\rho$	$\lambda_\perp$	$\in_\parallel$ (%)	G
−H	b(PH)	1.265/1.358	0.183184	−0.130922	0.537038	3.17	0.153962
$-BH_2$	b(PB)	2.163/1.535	0.156016	−0.394757	0.059490	5.74	0.011887
	b(BH)	0.955/1.286	0.185798	−0.238971	0.591839	23.97	0.140590
$-CH_3$	b(PC)	1.248/2.179	0.173744	0.053645	0.595439	4.29	0.183535
	b(CH)	1.255/0.794	0.284638	−1.041710	0.403043	1.39	0.048208
$-CHCH_2$	b(PC)	1.247/2.174	0.172107	0.075451	0.615608	0.27	0.185174
	b(CH)	1.259/0.782	0.291992	−1.108513	0.407250	0.08	0.044149
	b(CC′)	1.246/1.245	0.360706	−1.166583	0.196692	29.85	0.140871
	b(C′H′)	1.257/0.777	0.295897	−1.152305	0.412338	0.94	0.041103
	b(C′H″)	1.244/0.780	0.299679	−1.179736	0.408071	0.80	0.042547
	b(H″H″)	1.851/1.851	0.011077	0.041605	0.066357	4.25	0.008941
−CCH	b(PC)	1.229/2.110	0.168984	0.264306	0.824385	2.58	0.216162
	b(C-*nnm*)	0.818/0.392	0.414092	−0.594795	0.657491	0.18	0.582032
	b(*nnm*-C′)	0.194/0.843	0.418711	−0.896566	0.360075	0.68	0.515364
	b(C′H)	1.295/0.703	0.304276	−1.317743	0.391610	0.08	0.030241
	nnm		0.419961	−1.334389	0.316490		
−CN	b(PC)	1.235/2.125	0.164570	0.241830	0.786260	2.63	0.205595
	b(CN)	0.723/1.421	0.489588	0.968853	3.087650	0.01	1.104971
−CNO	b(PC)	1.232/2.090	0.162365	0.303923	0.835674	2.36	0.214001
	b(CN)	0.723/1.427	0.421826	2.010743	3.532558	0.18	1.147599
	b(NO)	1.124/1.104	0.543526	−1.137575	1.308783	0.10	0.450128
$-NH_2$	b(PN′)	1.190/1.963	0.178138	0.658832	1.305151	10.64	0.297810
	b(HN′)	0.456/1.424	0.355799	−1.940869	0.740906	5.27	0.058869
$-NHNH_2$	b(PN′)	1.194/1.942	0.171215	0.702558	1.313045	16.03	0.295616
	b(N′H)	1.418/0.457	0.362874	−1.983822	0.755471	7.64	0.061225
	b(N′N″)	1.346/1.317	0.317627	−0.686381	0.649791	19.08	0.131756
	b(N″H′)	1.416/0.443	0.365719	−2.010250	0.821600	9.33	0.060929
	b(N″H″)	1.399/0.446	0.372176	−2.035072	0.831005	9.65	0.064663
	b(H″H″)	1.644/1.644	0.014036	0.055298	0.092090	1.77	0.013007
−NC	b(PN′)	1.192/1.937	0.166688	0.755227	1.384068	0.77	0.297738
	b(CN′)	0.736/1.465	0.444112	0.354575	2.985299	0.15	0.852456
−NCS	b(PN′)	1.190/1.912	0.166067	0.816378	1.437184	0.64	0.308277
	b(NC′)	1.462/0.753	0.439174	0.067868	2.197741	0.08	0.787803
	b(CS)	1.841/1.124	0.224326	0.847041	1.263808	0.04	0.445802
$-N_3$	b(PN′)	1.211/1.982	0.162063	0.582470	1.137988	2.60	0.261528
	b(N′N″)	0.885/1.427	0.443259	−0.926998	0.388572	21.16	0.528485
	b(N″N‴)	1.302/0.771	0.616976	−1.815874	0.567105	12.40	0.955778
−OH	b(PO)	1.174/1.840	0.172696	1.036395	1.716117	4.96	0.352939
	b(HO)	0.335/1.443	0.383786	−2.459741	1.654141	1.37	0.081017
$-OCH_3$	b(PO)	1.174/1.821	0.171034	1.065845	1.729562	3.83	0.356219
	b(OC)	1.812/0.838	0.241607	0.114992	0.967224	2.86	0.376244
	b(CH)	1.273/0.768	0.302058	−1.201964	0.439321	5.15	0.037730
	b(CH)	1.264/0.781	0.299428	−1.172060	0.434539	5.51	0.039819
	b(HH)	2.313/2.313	0.007370	0.031426	0.039695	72.89	0.005921
−F	b(PF)	1.160/1.736	0.171896	1.361926	2.088694	0.33	0.405423
$-SiH_3$	b(PSi)	2.855/1.442	0.102949	0.002276	0.239733	2.14	0.073016
	b(SiH)	1.342/1.545	0.116080	0.298418	0.656073	2.49	0.140194
$-PH_2$	b(PP′)	2.193/2.007	0.128510	−0.224074	0.093825	7.50	0.016606
	b(P′H)	1.259/1.391	0.164857	0.091729	0.567333	12.12	0.180327
−SH	b(PS)	1.707/2.276	0.144167	−0.316934	0.061000	5.79	0.028588
	b(SH)	1.289/1.212	0.223719	−0.549556	0.075088	22.67	0.143721
−SCN	b(PS)	1.785/2.242	0.137643	−0.266739	0.094476	7.45	0.025652
	b(SC)	1.219/1.989	0.209230	−0.121547	0.354176	35.55	0.220435
	b(CN)	0.724/1.422	0.484796	0.970457	2.925029	4.26	1.097502
	b(CC)	3.034/3.034	0.007904	0.026091	0.034003	55.10	0.005326
−Cl	b(PCl)	1.323/2.456	0.146587	−0.090895	0.307065	5.15	0.120470
−Br	b(PBr)	1.517/2.574	0.135885	−0.298990	0.035285	5.43	0.047489

[a] All critical points but those forming the $(NP)_3$ ring are given in this table. The notation and units follow the conventions in Table 5.

Jemmis and Kiran determined the ASE for $[NPH_2]_3$ to be 9.3 kcal/mol, the cyclotriphosphazene being more stable, by means of B3LYP/6-31G* calculations. Our HF/6-31G** calculations predict and ASE of 42.4 kcal/mol for the same compound, the difference with the Jemmis and Kiran result being due to the absence of basis set superposition correction and electronic correlation from our calculations. As a comparison, our ASE values for $[NPCl_2]_3$ and $[NPF_2]_3$ are −9.3 and −17.7 kcal/mol, respectively, which indicates that the cyclotriphosphazenes are not energetically favored in reaction 9.

A different evidence of the lack of aromaticity rests on the evolution of the cyclophosphazene properties with the ring size. Table 9 presents the geometry and topological properties of $[NPCl_2]_n$ for n: 2−5. The total energy per $NPCl_2$ group remains very similar in the different rings, decreasing slightly (i.e., increasing the stability) as n passes from 3 to 5. At the same time, the PN distance decreases and the PN bond critical points increase their electron density and Laplacian. Every property shows a smooth evolution with the ring size and no sign of special properties for those systems satisfying the $4n + 2$ rule is found.

A most interesting fact is, perhaps, the different behavior of the NPN and PNP ring angles. Whereas the NPN angle remains almost constant, the PNP angle opens considerably as the ring

TABLE 7: Topological Properties of Bond and Ring Critical Points of the Electron Density of Several Molecules Containing PN Bonds[a]

molecule	CP	r_i/r_j	ρ	$\nabla^2\rho$	$\lambda_\perp$	$\epsilon_\parallel$ (%)	G
$NPCl_2$	b(PN)	1.119/1.659	0.241287	1.614006	2.233957	14.89	0.596058
	b(PCl)	1.342/2.438	0.142687	−0.094275	0.264486	10.92	0.111630
$ClNPCl_3$	b(PN)	1.139/1.776	0.226823	1.129689	1.857216	22.80	0.471322
	b(PCl)	1.311/2.432	0.152192	−0.078625	0.335999	4.90	0.129848
	b(NCl)	1.592/1.639	0.214402	−0.306898	0.366206	1.51	0.091530
	b(PCl)	1.348/2.455	0.144060	−0.131171	0.238256	1.46	0.107222
Cl_2NPCl_4	b(PN)	1.227/2.011	0.157650	0.477406	0.953133	9.53	0.236452
	b(Cl″N)	1.556/1.678	0.214622	−0.318736	0.333036	5.77	0.098813
	b(Cl″Cl)	2.763/2.802	0.020763	0.088554	0.118172	10.42	0.019660
	b(PCl)	1.643/2.388	0.123440	−0.220748	0.079926	3.02	0.038215
	b(PCl′)	1.421/2.444	0.142538	−0.254364	0.100154	8.61	0.074122
	r(Cl″NPCl)		0.018309	0.093358	−0.013319	76.87	0.019632

[a] Magnitudes and units follow the Table 5 notation.

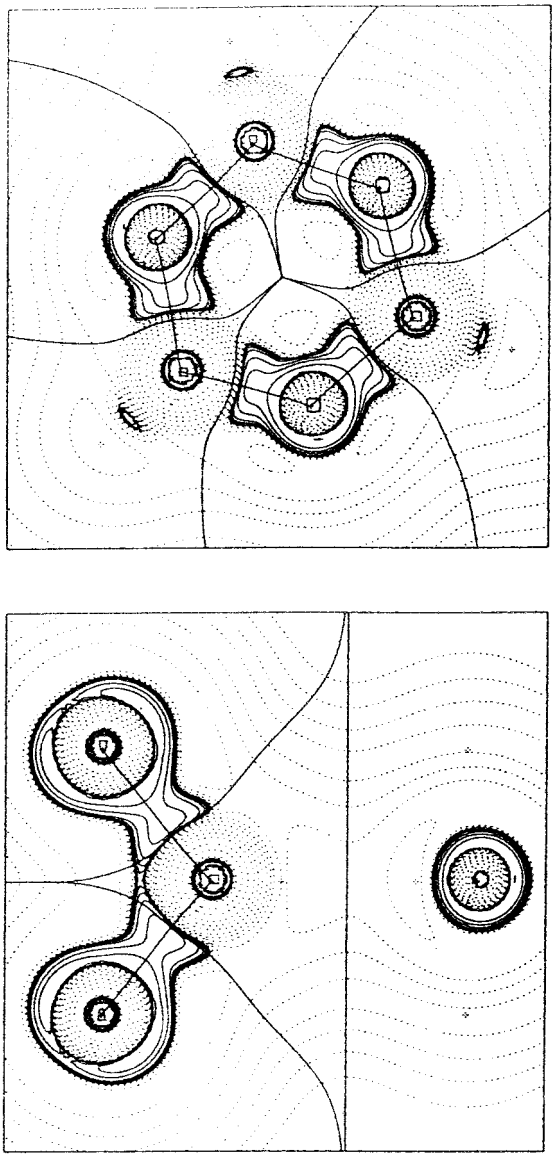

Figure 1. Laplacian scalar field of $[NPCl_2]_3$ on the ring plane (top), a $NPCl_2$ plane (bottom). Regions with negative values of $\nabla^2\rho$ appear as continuous contour lines, whereas dashed lines are used for $\nabla^2\rho >$ 0 contours. The contours depicted follow a logarithmic-like scale: ± 0.001, and ± 2, ± 4, $\pm 8 \times 10^n$ e/bohr^3 with n: (−3)−(+2). The gradient lines starting on the in-plane bond critical points are also plotted to show the molecular graph and the frontier among atomic basins.

passes from $n = 3$ to $n = 5$. This phenomenon is also well established experimentally in the methylcyclophosphazenes, $[NP(CH_3)_2]_n$, where rings of size n: 3−12 have been studied[60] to find that the PNP angle widens from 122.6° at the $n = 3$ ring to 132.9° at the $n = 5$ ring, the larger rings being increasingly distorted out from planarity. We should conclude that the PNP angle is softer and easier to deform than the NPN angle. This can be confirmed directly by determining the total energy of the two model molecules:

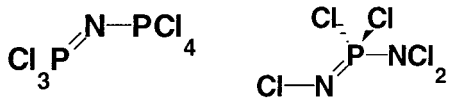

4 5

as a function of the PNP and NPN angles, respectively. The optimal PNP angle found for the first molecule is 173.83°, and the force constant obtained for the change of this bond angle is 2.036×10^{-6} hartree/deg^2. Equivalently, the second molecule presents an optimal NPN angle of 122.03° and a force constant of 66.97×10^{-6} hartree/deg^2, more than 30 times that for the bending of the PNP angle.

We have already seen that the *XPX* angle varies largely depending on the size and electronegativity of the *X* functional group (see Table 3). The size of the ring, on the other hand, appears not to have a significant influence on this angle, as the data in Table 9 and in ref 60 indicates. *Why are the ClPCl and the MePMe angles so constant and yet so different?* The shape of the Cl basins depicted in Figure 1b for the plane containing the ClPCl angle helps with the explanation. The Cl basins approach to the point of being almost in contact. It must be stressed, however, that no true contact exist among them because no ClCl bond critical point occurs in the $[NPCl_2]_n$ phosphazenes. The ClPCl angle is then determined by the nonbonding contact among the Cl basins and an equivalent thing happens for the remaining functional groups that we have examined. In fact, the principle that the secondary geometry is determined by the nonbonding contact of ligands appears to be quite general and it is discussed at length in refs 61−63.

C. The Lewis Model and Beyond. We will turn now to examine the degree of electron pairing in the phosphazene bonding in terms of the localization and delocalization indices defined in section 2.

An electron pair equally shared between two centers A and B would add both to the localization indices λ(A) and λ(B), and to the delocalization index δ(A,B). As an example, in H_2 λ(H) = 0.5 and δ(H,H) = 1, meaning that an electron pair is equally shared between the two hydrogen atoms. A further example is N_2, for which a good Hartree−Fock wave function produces λ(N) = 5.48 and δ(N,N) = 3.04.[39] When the two centers *A* and *B* differ in electronegativity, on the other hand,

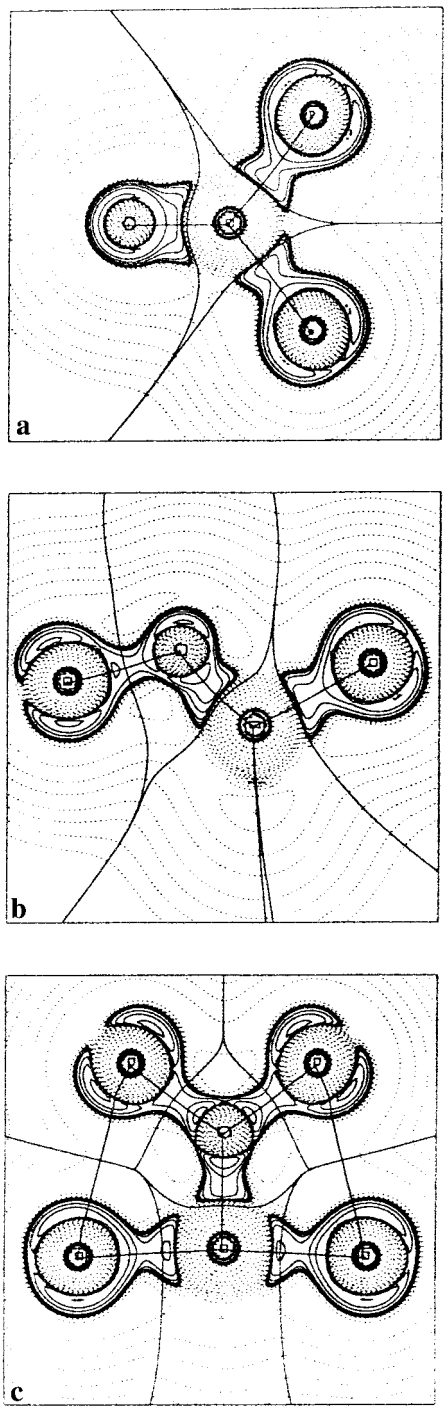

Figure 2. Laplacian scalar field representation of some significant molecules: (a) $NPCl_2$, (b) $ClNPCl_3$, and (c) Cl_2NPCl_4. The contours follow the description in Figure 1.

the shared electron pairs contribute unequally to λ(A), λ(B) and δ(A,B). In the limit of purely ionic bonding the electron pair would be totally localized to the anion and would approach zero. This is what happens in LiF, where $\lambda(\mathrm{Li}) = 1.97$, $\lambda(\mathrm{F}) = 9.85$, and $\delta(\mathrm{Li,F}) = 0.18$.[39]

Our Hartree−Fock results for some relevant phosphazene molecules are presented in Figure 4. The NP bond in $[NPCl_2]_3$ has a significant ionicity and $\delta(\mathrm{N,P}) = 0.63$, a value wich is much smaller than that found for a formal double bond (0.85) and only slightly larger than that of a formal single bond (0.60). All six NP bonds in the cyclophosphazene ring are again identical. The PCl bonding also shows a significant degree of

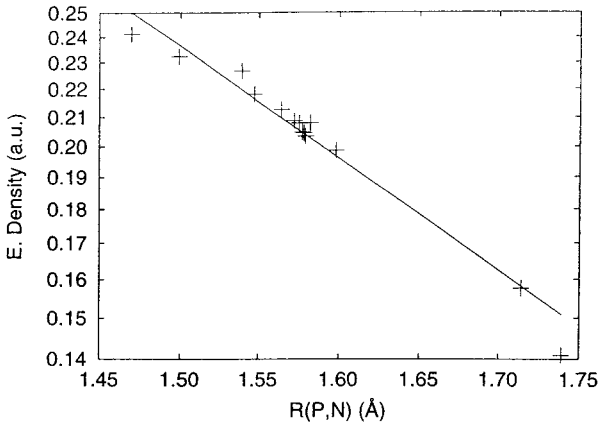

Figure 3. Electron density at the PN bond critical point for the molecules in Tables 5 and 7. Notice the logarithmic scale for the density.

TABLE 8: Topological Charges of the Atoms in the Clyclotriphosphazenes $[NPX_2]_3$

−*XYZRS*	*Q*(N)	*Q*(P)	*Q*(*X*)	*Q*(*Y*)	*Q*(*Z*)	*Q*(*R*)	*Q*(*S*)
−H	−2.299	3.597	−0.647				
$-BH_2$	−2.317	1.910	1.617	−0.705			
$-CH_3$	−2.349	3.675	−0.549	−0.038			
−CHCHH	−2.337	3.690	−0.686	−0.023	0.019	−0.027	−0.040
−CCH	-						
−CN	−2.307	3.808	0.596	−1.344			
−CNO	−2.316	3.831	0.371	−0.693	−0.435		
$-NH_2$	−2.370	3.902	−1.650	0.443			
−NHNHH	−2.356	3.903	−1.238	0.431	−0.866	0.459	0.444
−NC	−2.328	3.949	1.277	−2.086			
−NCS	−2.333	3.959	−2.008	0.680	0.514		
$-N_3$	−2.333	3.880	−0.763	−0.475	0.467		
−OH	−2.340	3.986	−1.477	0.657			
$-OCH_3$	−2.350	3.961	−1.493	0.769	−0.029		
−F	−2.317	4.040	−0.861				
$-SiH_3$	−2.312	1.042	2.851	−0.738			
$-PH_2$	−2.327	2.177	1.272	−0.597			
−SH	−2.318	2.885	−0.029	−0.253			
−SCN	−2.302	2.788	0.328	0.800	−1.370		
−Cl	−2.313	3.556	−0.621				
−Br	−2.306	3.226	−0.457				

unequal sharing and $\delta(\mathrm{P,Cl}) = 0.58$. It is very interesting to observe that the sharing of electron pairs is not limited to those atoms directly linked in the chemical graph. In fact, the nitrogen atoms in the phosphazene ring have a nonnegligible $\delta(N,N) = 0.20$, even if they are not linked by a bond path. On the contrary, the phosphorus atoms show a negligible sharing (less that 0.01). Sharing is also observable between the nearest N and Cl pairs and between two Cl atoms linked to the same P. The delocalization index, thus, provides an information that complements and is not simply contained in the image provided by the electron density topological field.

A comparison with benzene is in order to reveal the big differences among the C_6 and $[NP]_3$ rings. The HF/6-31G* wave function of benzene predicts the following values for the CC delocalization indices: 1.39 (between two C atoms in orto position), 0.07 (atoms in meta), 0.10 (atoms in para). Sharing occurs here mainly among nearest neighbors, with a small but significant sharing distributed across the whole C_6 ring. By contrast, the PN bond presents a large ionic component and, accordingly, a much reduced pair sharing. Sharing across the ring is negligible except for the N_3 group formed by the N atoms in meta.

The traditional Lewis structure of a $[NPX_2]_3$ compound involves a $(sp_2)^4(p)^1$ hybridization on N and a $(sp_3d)^5$ hybridization of P. This is in accordance with the ≈120° angles in the

TABLE 9: Equilibrium Geometry and Main Topological Properties of $[NPCl_2]_n$ Cyclophosphazenes Obtained from Our HF/6-31G Calculations[a]**

n	ϵ	PN	NPN	PNP	PCl	ClPCl	ρ_b(PN)	$\nabla^2\rho_b$(PN)
2	−0.145023	1.623	95.880	84.120	1.992	102.900	0.203152	0.757464
3	−0.183641	1.577	116.240	123.760	2.000	102.767	0.204819	0.992607
		(1.581)[b]	(118.4)	(121.4)		(101.3)		
4	−0.186741	1.550	120.255	149.650	2.007	103.064	0.206899	1.131737
		(1.57)[c]	(120.5)	(137.6)		(102.8)		
5	−0.186997	1.537	119.510	168.242	2.009	103.117	0.209458	1.206858
		(1.52)[d]	(118.4)	(148.6)		(102.2)		

[a] In the table $\epsilon = E_{HF}/n + 1314$ hartree. Experimental values, where available, are given in parentheses. Distances are given in angstroms, angles in degrees, and topological properties in atomic units. [b] Reference 71. [c] Reference 68. [d] Reference 68.

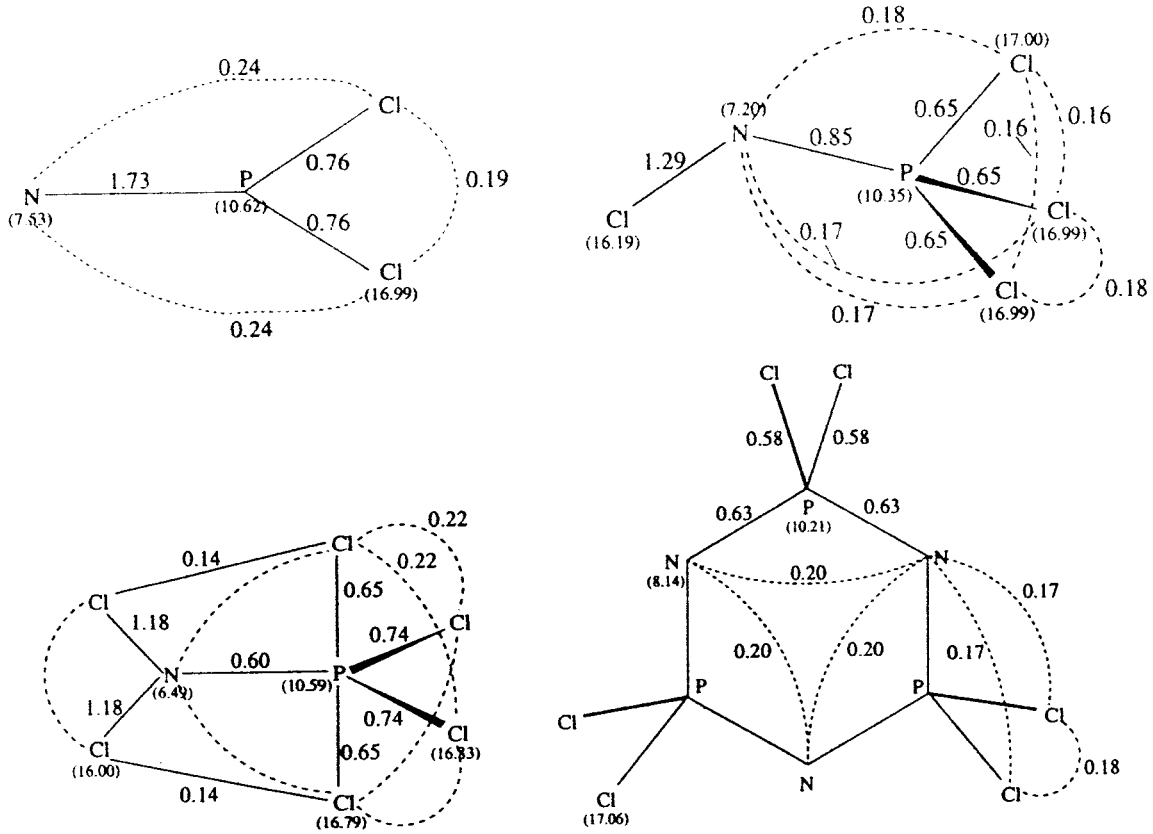

Figure 4. Atomic localization ($\lambda(A)$, in parentheses) and bond delocalization (δ(A,B), on the interatomic lines) indices obtained in the HF/6-31G** calculation of (a) $NPCl_2$, (b) $ClNPCl_3$, (c) Cl_2NPCl_4, and (d) $[NPCl_2]_3$. Solid lines correspond to true bond paths whereas dashed lines indicate sharing of more that δ(A,B) = 0.12 but no bond path. All values are given in atomic units.

phosphazene ring, the coordination four on P and the formation of three π N−P bonds in the ring. In addition, it also predicts the occurrence of a lone pair on each N located in the plane and directed outward from the phosphazene ring.

The details of the involvement of the d orbitals of phosphorus in the formation of the d_π(P)−p_π(N) bonds remain, however, the subject of an old debate. Craig et al.[64−66] first proposed the heteromorphic interaction of tangentially directed d_{xz} P orbitals with the N p_z, resulting in an aromatic π system with the topology of a Møbius strip. Dewar et al.[16] proposed a combination of homo- and heteromorphic interactions with the result that both d_{xz} and d_{yz} P orbitals would participate in forming a three-center two-electron bonding system showing characteristic islands of delocalization and no aromaticity. Within this context, Ferris et al.[9−11] recognized the influence of the *X* groups and discussed the P → N charge transfer due to the difference in electronegativity between both atoms.

This old debate is not solved but surpassed by the AIM theory. Molecular orbitals in closed shell systems, although essentially involved in our most rigorous methods to solve the molecular electronic structure, can be arbitrarily changed by means of unitary transformations without modifying any observable property of the molecule. Therefore, molecular orbitals have no significance for the molecular bonding, as far as it may be related to physically measurable quantities. The electron density, on the other hand, is an observable property and the topological features of the Laplacian $\nabla^2\rho$ can be related to the traditional bonded and nonbonded pairs in Lewis's model, thus avoiding the need to invoke any nonmeasurable and arbitrary property.

Regions with negative (positive) value of $\nabla^2\rho$ occur where the electron density is locally concentrated (depleted), as compared to the adjacent points. The form of $\nabla^2\rho$ for an isolated atom reflects the shell structure by exhibiting a number of pairs of spherical shells of alternating charge concentration and depletion. Upon chemical combination the outer valence shell of charge concentration is distorted and, eventually, the valence shell from an atom can be lost due to charge transfers to other centers in the molecule. This is exactly what happens in the phosphazenes, where the outer shells of the ring P atoms disappear due to the P → N and P → *X* charge transfer.

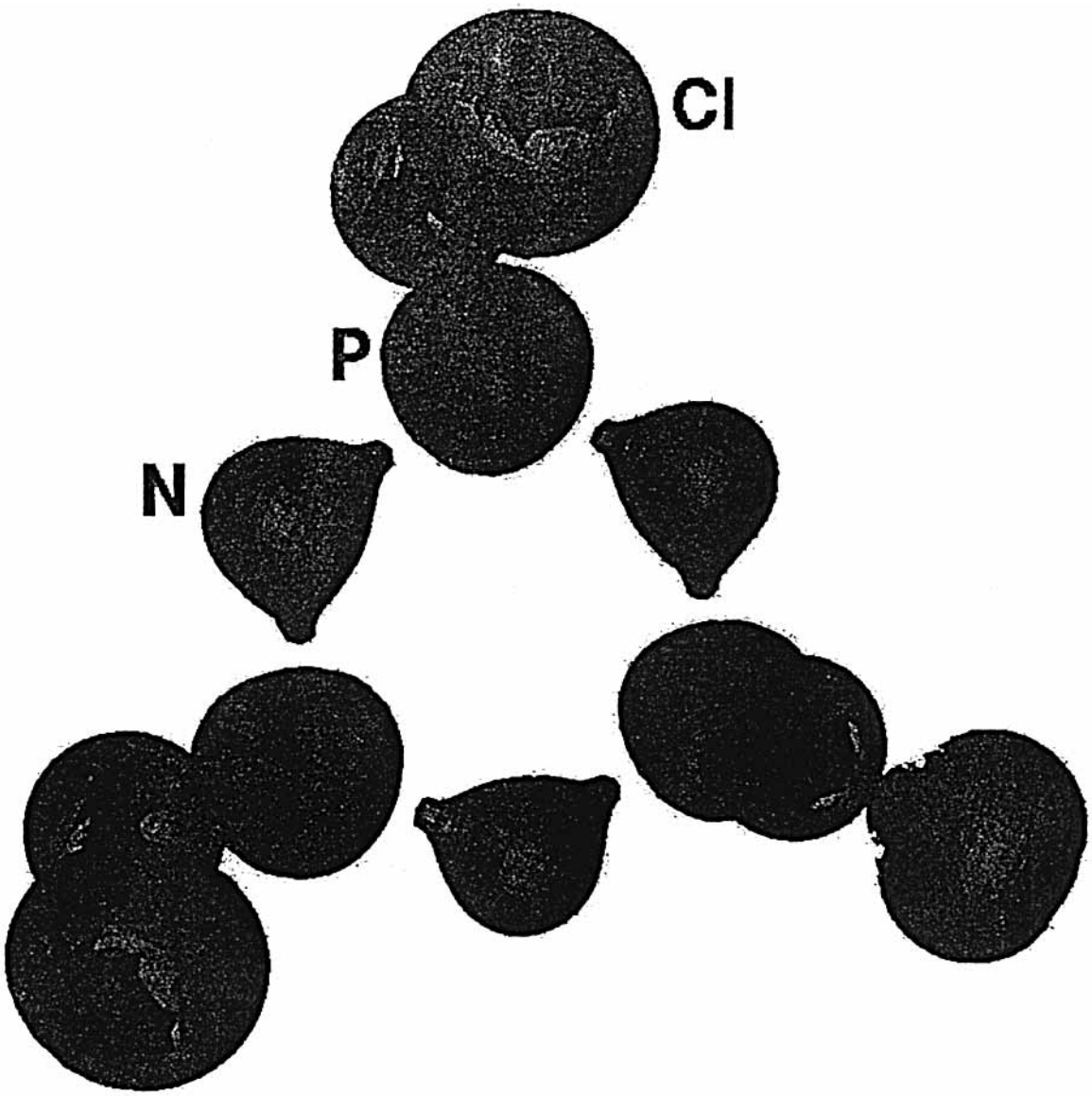

Figure 5. Isosurfaces of $\nabla^2\rho(\vec{r})$ in $[NPCl_2]_3$. The surfaces of -0.5 *e*/bohr^5 are depicted in a light tone whereas dark areas depict the $+0.5$ *e*/bohr^5 isosurface.

The electrophilic and nucleophilic regions in a molecule can be globally revealed in a three-dimensional isosurface map of $\nabla^2\rho$. Such a map is depicted in Figure 5 for $[NPCl_2]_3$. Ring N atoms are shown to wear a large valence shell of charge concentration whereas ring P atoms are dressed in a charge depletion shell. Therefore, ring N and P atoms are electron rich and electron poor zones entitled to suffer electrophilic and nucleophilic attacks, respectively. This difference among both atoms lies at the core of the main reactivity of phosphazene compounds.[4] The $\nabla^2\rho$ isosurface maps of all cyclotriphosphazenes are essentially identical as far as the aspect of the $(NP)_3$ ring is concerned. The maps provide, however, an excellent view of the differences among the functional groups attached to the ring.

The comparison among compounds is easier to do quantitatively by enlisting and analyzing the topological features of $\nabla^2\rho$. The (3,+3) critical points of the Laplacian identify bonded and nonbonded charge concentrations. The former correspond to points which lie on a bond path linking two atoms, while the latter are located on the valence shell of a given atom and correspond to the electron lone pairs.[35,67] It has been shown that a good linear relationship occurs between the intrinsic basicity and the charge density at the basic center lone pair:[68] the greater the charge density associated with the lone pair the easier is the charge transfer to the incoming electrophile, be it a bare proton or a more complex reactive group.

Table 10 presents the most characteristic lone pairs found in the Laplacian field of the cyclotriphosphazenes. The close resemblance between all ring N lone pairs is here quantitatively confirmed. A single (3,+3) lone pair is associated with each ring N atom, situated at a distance of 0.75−0.76 bohr and showing an electron density of 0.482−0.506 *e*/bohr^3. This electron density is significantly smaller than the values found for N in the −CN (0.600 *e*/bohr^3) and $-NH_2$ (0.554 *e*/bohr^3) groups, but equivalent to N in the $-N_3$(0.468 *e*/bohr^3) group. It is also smaller than the densities at the F and O (either in the −CNO, −OH, or $-OCH_3$ groups) atoms lone pairs, similar to the lone pairs on Cl, and larger than those on Br and P in the PH_2 group. Accordingly, ring N atoms are expected to behave as weak Lewis bases and show a rather constant intrinsic basicity, almost independent from the ligands attached to the ring.

It is interesting to observe, finally, that some atoms exhibit more that one (3,+3) lone pair. This is the case of the O atom

TABLE 10: (3,+3) Most Significant Critical Points of $\nabla^2\rho$ in the $[NPX_2]_3$ Cyclophosphazenes[a]

$-X$	atom A	R(CP$-A$)	ρ(CP)	$\nabla^2\rho$	
$-H$	N(ring)	0.750	0.496	-2.120	
$-BH_2$	N(ring)	0.758	0.492	-1.978	
$-CH_3$	N(ring)	0.759	0.489	-1.937	
$-CHCH_2$	N(ring)	0.758	0.492	-1.976	
$-CCH$	N(ring)	0.756	0.495	-1.994	
$-CN$	N(CN)	0.723	0.600	-3.604	
	N(ring)	0.754	0.498	-2.022	
$-CNO$	O	0.640	0.920	-5.547	
	N(ring)	0.755	0.498	-2.024	
$-NH_2$	N(NH_2)	0.741	0.554	-2.751	
	N(ring)	0.762	0.482	-1.828	
	N(NH_2)	0.766	0.491	-1.856	
$-NHNH_2$	N(ring)	0.754	0.504	-2.116	
$-NC$	N(ring)	0.754	0.499	-2.029	
	C	0.859	0.324	-1.476	
$-NCS$	N(ring)	0.755	0.498	-2.028	
$-N_3$	N(ring)	0.756	0.496	-2.008	
	N(N_3)	0.797	0.468	-1.738	
$-OH$	O	0.638	0.952	-5.826	$\times 2$
	N(ring)	0.756	0.496	-2.008	
$-OCH_3$	O	0.638	0.955	-5.814	
	N(ring)	0.758	0.492	-1.962	
-F	F	0.558	1.516	-10.671	$\times 2$
	F	0.558	1.514	-10.617	(3,+1) LCP
	N(ring)	0.754	0.498	-2.021	
$-SiH_3$	N(ring)	0.795	0.488	-1.934	
$-PH_2$	N(ring)	0.759	0.489	-1.946	
	P(PH_2)	1.441	0.129	-0.306	
$-SH$	N(ring)	0.753	0.505	-2.116	
	S	1.292	0.195	-0.540	$\times 2$
$-SCN$	N(ring)	0.753	0.506	-2.121	
$-Cl$	N(ring)	0.754	0.502	-2.072	
	Cl	1.171	0.276	$-0-0.818$	$\times 2$
	Cl	1.172	0.275	-0.810	
$-Br$	N(ring)	0.753	0.503	-2.089	
	Br	1.562	0.168	-0.126	$\times 2$
	Br	1.563	0.167	-0.124	

[a] R(CP$-A$) is the distance from the nucleus to the critical point. All properties are given in au.

in $-$OH and $-OCH_3$, which have two pairs, and of the Cl and Br groups, which have three pairs each. The F group, with only two (3,+3) lone pairs, appears to deviate from the other halogens but a more careful inspection reveals the third lone pair converted into a (3,+1) critical point of $\nabla^2\rho$ with properties almost identical to the two other pairs.

V. Summary

The topology of the electron density of some 27 phosphazene derivatives has been presented and discussed. The HF/6-31G** geometries agree with the experimental data to about 0.01 Å and 1$-$2°. The equilibrium geometry and bonding properties of the cyclophosphazene ring are very constant in all the $[NPX_2]_3$ compounds. The NPN angle is rather stiff whereas the PNP angle is much softer, the *XPX* angle being determined by the nonbonding contact among the *X* substituents. The PN bond is strong, highly polarized, and involves a large electron transfer from P to N. The charge on the P atoms depends heavily on the electronegativity of the *X* substituent, while that on the ring N atoms remains nearly constant in all cyclotriphosphazenes. The delocalization indices show a small sharing of about 0.7 electron pairs between bonded N and P atoms. Sharing across the ring is negligible except for the N_3 group formed by the N atoms in meta. Aromaticity is then absent from the cyclophosphazene rings, which agrees well with the indiscriminated stability of rings of different size. Finally, ring N and P atoms are electron rich and electron poor zones ready to suffer electrophilic and nucleophilic attacks, respectively.

Acknowledgment. Financial support from the DGICYT, Projects PB96-0559 and PB98-1276, is hereby acknowledged.

References and Notes

(1) Allcock, H. R. *Chem. Rev.* **1972**, *72*, 315.
(2) Allcock, H. R. *Phosphorus−Nitrogen Compounds. Cyclic, Linear and High Polymeric Systems*; Academic: New York, 1972.
(3) Allen, C. W. *Coord. Chem. Rev.* **1994**, *130*, 137.
(4) Allen, C. W. *Chem. Rev.* **1991**, *91*, 119.
(5) Mark, J. E.; Allcock, H. R.; West, R. *Inorganic Polymers*; Prentice Hall: New York, 1992.
(6) Manners, I. *Angew. Chem., Int. Ed. Engl*. **1996**, *35*, 1602.
(7) de Jaeger, R.; Gleria, M. *Prog. Polym. Sci*. **1998**, *23*, 179.
(8) Trinquier, G. *J. Am. Chem. Soc*. **1986**, *108*, 568.
(9) Ferris, K. F.; Friedman, P.; Friedrich, D. M. *Int. J. Quantum Chem.: Quantum Chem. Symp*. **1988**, *22*, 207.
(10) Ferris, K. F.; Duke, C. B. *Int. J. Quantum Chem.: Quantum Chem. Symp*. **1989**, *23*, 397.
(11) Dake, L. S.; Baer, D. R.; Ferris, K. F.; Friedrich, D. M. *J. Electron Spectrosc. Related Phenom*. **1990**, *51*, 439.
(12) Cameron, T. S.; Borecka, B.; Kwiatkowski, W. *J. Am. Chem. Soc.* **1994**, *116*, 1211.
(13) Jaeger, R.; Debowski, M.; Manners, I.; Vancso, G. J. *Inorg. Chem.* **1999**, *38*, 1153.
(14) Breza, M. *Polyhedron* **2000**, *19*, 389.
(15) Greenwood, N. N.; Earnshaw, A. *Chemistry of the Elements*, 2nd ed.; Butterworth-Heinemann: Oxford, UK, 1998.
(16) Dewar, M. J. S.; Lucken, E. A. C.; Whitehead, M. A. *J. Chem. Soc*. **1960**, 2423.
(17) Bader, R. F. W. *Atoms in Molecules—A Quantum Theory*; Oxford University Press: Oxford, 1990.
(18) Bader, R. F. W. *Int. J. Quantum Chem.* **1995**, *56*, 409.
(19) Bader, R. F. W. *Phys. Rev. B* **1994**, *49*, 13348.
(20) Bader, R. F. W. *Int. J. Quantum Chem.* **1994**, *49*, 299.
(21) Bader, R. F. W.; Popelier, P. L. A. *Int. J. Quantum Chem.* **1993**, *45*, 189.
(22) Zou, P. F.; Bader, R. F. W. *Int. J. Quantum Chem.* **1992**, *43*, 677.
(23) Bader, R. F. W. *Chem. Rev.* **1991**, *91*, 893.
(24) Bader, R. F. W. *J. Chem. Phys.* **1989**, *91*, 6989.
(25) Bader, R. F. W. *Prog. Appl. Chem.* **1988**, *60*, 145.
(26) Bader, R. F. W.; Macdougall, P. J. *J. Am. Chem. Soc.* **1985**, *107*, 6788.
(27) Bader, R. F. W. *Acc. Chem. Res.* **1985**, *18*, 9.
(28) Bader, R. F. W.; Essen, H. *J. Chem. Phys.* **1984**, *80*, 1943.
(29) Bader, R. F. W.; Nguyen-Dang, T. T.; Tal, Y. *Rep. Prog. Phys.* **1981**, *44*, 893.
(30) Bader, R. F. W.; Nguyen-Dang, T. T. *Adv. Quantum Chem.* **1981**, *14*, 63.
(31) Bader, R. F. W.; Srebrenik, S.; Nguyen-Dang, T. T. *J. Chem. Phys.* **1978**, *68*, 3680.
(32) Srebrenik, S.; Bader, R. F. W.; Nguyen-Dang, T. T. *J. Chem. Phys.* **1978**, *68*, 3667.
(33) Bader, R. F. W. *Acc. Chem. Res.* **1975**, *8*, 34.
(34) Bader, R. F. W. *J. Phys. Chem. A* **1998**, *102*, 7314.
(35) Bader, R. F. W.; Macdougall, P. J.; Lau, C. D. H. *J. Am. Chem. Soc.* **1984**, *106*, 1594.
(36) Lewis, G. N. *J. Am. Chem. Soc.* **1916**, *38*, 762.
(37) Bader, R. F. W.; Johnson, S.; Tang, T. H.; Popelier, P. L. A. *J. Phys. Chem.* **1996**, *100*, 15398.
(38) Bader, R. F. W.; Streitwieser, A.; Neuhaus, A.; Laidig, K. E.; Speers, P. *J. Am. Chem. Soc.* **1996**, *118*, 4959.
(39) Fradera, X.; Austen, M. A.; Bader, R. F. W. *J. Phys. Chem. A* **1999**, *103*, 304.
(40) Bader, R. F. W.; Stephens, M. E. *J. Am. Chem. Soc.* **1975**, *97*, 7391.
(41) M. W. Schmidt et al., *J. Comput. Chem.* **1993**, *14*, 1347.
(42) Bader's Laboratory, R. W. F. *AIMPAC*; 1989. See the code home page at http://www.chemistry.mcmaster.ca/aimpac/.
(43) Schaftenaar, G. *Molden*; 1996. See the home page at http://www.caos.kun.nl/schaft/molden/molden.html.
(44) Luaña, V. *Tessel, version 2.1*; 2000. See the program web page at http://www.uniovi.es/quimica.fisica/qcg/src/tessel.html.
(45) Anger, S.; Bayer, D.; Cason, C.; Dilger, C. D. A.; Demlow, S.; Enzmann, A.; Wegner, D. F. T.; Young, C. *POV−Ray: Persistence of the Vision Ray Tracer*; 1997. See the POV−Ray WWW home page at http://www.povray.org.

(46) Phillips, M.; Munzner, T.; Levy, S. *Geomview*; The Geometry Center, University of Minnesotta: St. Paul, 1995. Available via anonymous ftp from geom.umn.edu.
(47) Hehre, W. J.; Radom, L.; Pople, J. A.; Schleyer, P. v. R. *Ab Initio Molecular Orbital Theory*; Wiley: New York, 1986.
(48) Bader, R. F. W.; Biegler-König, F. W.; Tal, Y.; Tang, T. H. *J. Am. Chem. Soc.* **1982**, *104*, 946.
(49) Boyd, R. J. *J. Stud. Org. Chem. (Amsterdam)* **1987**, *31*, 485.
(50) Knop, O.; Boyd, R. J.; Choi, S. C. *J. Am. Chem. Soc.* **1988**, *110*, 7299.
(51) Gibbs, G. V.; Tamada, O.; Boisen, M. B. *Phys. Chem. Mineral.* **1997**, *24*, 432.
(52) Gibbs, G. V.; Hill, F. C.; Boisens, M. B.; Downs, R. T. *Phys. Chem. Miner*. **1998**, *25*, 585.
(53) Pendás, A. M.; Costales, A.; Luaña, V. *J. Phys. Chem. B* **1998**, *102*, 6937.
(54) Espinosa, E.; Souhassou, M.; Lachekar, H.; Lecomte, C. *Acta Crystallogr. B* **1999**, *55*, 563.
(55) Cioslowski, J.; Edgington, L.; Stefanov, B. B. *J. Am. Chem. Soc*. **1995**, *117*, 10381.
(56) Bader, R. F. W. *J. Phys. Chem A* **1998**, *102*, 7314.
(57) Pendás, A. M.; Blanco, M. A.; Costales, A.; Mori-Sánchez, P.; Luaña, V. *Phys. Rev. Lett*. **1999**, *83*, 1930.
(58) Keith, T. A.; Bader, R. F. W. *J. Chem. Phys.* **1993**, *99*, 3669.
(59) Jemmis, E. D.; Kiran, B. *Inorg. Chem.* **1998**, *37*, 2110.
(60) Oakley, R. T.; Rettig, S. J.; Paddock, N. L.; Trotter, J. *J. Am. Chem. Soc*. **1985**, *107*, 6923.
(61) Gillespie, R. J.; Johnson, S. A. *Inorg. Chem.* **1997**, *36*, 3031.
(62) Gillespie, R. J.; Bytheway, I.; Robinson, E. A. *Inorg. Chem.* **1998**, *37*, 2811.
(63) Gillespie, R. J.; Robinson, E. A.; Heard, G. L. *Inorg. Chem.* **1998**, *37*, 6884.
(64) Craig, D. P.; Paddock, N. L. *J. Chem. Soc*. **1962**, 4118.
(65) Craig, D. P.; Mitchell, K. A. R. *J. Chem. Soc*. **1965**, 4682.
(66) Paddock, N. L. *Q. Rev., Chem. Soc*. **1964**, *18*, 168.
(67) Bader, R. F. W.; Chang, C. *J. Phys. Chem.* **1989**, *93*, 2946.
(68) Ijjaali, F.; Mo, O.; Yañez, M.; Abboud, J. L. M. *J. Mol. Struct. (THEOCHEM)* **1995**, *338*, 225.
(69) Dougill, M. W. *J. Chem. Soc*. **1962**, 3211.
(70) Singh, R. P.; Vij, A.; Kirchmeier, R. L.; Shreeve, J. M. *Inorg. Chem.* **2000**, *39*, 375.
(71) Bullen, G. J. *J. Chem. Soc. A* **1971**, 1450.
(72) Oakley, R. T.; Paddock, N. L.; Rettig, S. J.; Trotter, J. *Can. J. Chem*. **1977**, *55*, 4206.
(73) Golinski, F.; Jacobs, H. Z. *Anorg. Allg. Chem.* **1994**, *620*, 965.
(74) Faught, J. B.; Moeller, T.; Paul, I. C. *Inorg. Chem.* **1970**, *9*, 1656.
(75) Giglio, E.; Puliti, R. *Acta Crystallogr*. **1967**, *22*, 304.
(76) de Santis, P.; Giglio, E.; Ripamonti, A. *J. Inorg. Nucl. Chem*. **1962**, *24*, 469.
(77) Zoer, H.; Wagner, A. J. *Acta Crystallogr. B* **1970**, *26*, 1812.
(78) Wagner, A. J.; Vos, A. *Acta Crystallogr. B* **1968**, *24*, 707.
(79) Schlueter, A. W.; Jacobson, R. A. *J. Chem. Soc. A* **1968**, 2317.